Downregulation of an *Entamoeba histolytica* rhomboid protease reveals roles in regulating parasite adhesion and phagocytosis

Leigh A. Baxt,[1] Elena Rastew,[1] Rivka Bracha,[2] David Mirelman,[2] and Upinder Singh[1,3]

[1]Department of Microbiology and Immunology, Stanford University School of Medicine, Stanford, CA 94305, USA.

[2]Department of Biological Chemistry, Weizmann Institute of Science, Rehovot 76100, Israel.

[3]Department of Internal Medicine, Division of Infectious Diseases, S-143 Grant Building, 300 Pasteur Drive, Stanford, CA, 94305

Corresponding author: Email: usingh@stanford.edu

Telephone: 650-723-4045

Fax: 650-724-3892

1

ABSTRACT

Entamoeba histolytica is a deep-branching eukaryotic pathogen. Rhomboid proteases are intramembrane serine protease, which cleave transmembrane proteins in, or in close proximity to, their transmembrane domain. We have previously shown that *E. histolytica* contains a single functional rhomboid protease (EhROM1), with unique substrate specificity. EhROM1 is present on the trophozoite surface and relocalizes to internal vesicles during erythrophagocytosis and to the base of the cap during surface receptor capping. In order to further examine the biological function of EhROM1 we downregulated EhROM1 expression by >95% by utilizing the epigenetic silencing mechanism of the G3 parasite strain. Despite the observation that EhROM1 re-localized to the cap during surface receptor capping, EhROM1 knockdown (ROM(KD)) parasites had no gross changes in cap formation or complement resistance. However, ROM(KD) parasites demonstrated decreased host cell adhesion, a result recapitulated by treatment of wild-type parasites with DCI, a serine protease inhibitor with activity against rhomboid proteases. The reduced adhesion phenotype of ROM(KD) parasites was noted exclusively with healthy cells, but not with apoptotic cells. Additionally, ROM(KD) parasites had decreased phagocytic ability with reduced ingestion of healthy cells, apoptotic cells and rice starch. Decreased phagocytic ability is thus independent of the reduced adhesion phenotype, since phagocytosis of apoptotic cells was reduced despite normal adhesion levels. The defect in host cell adhesion was not explained by altered expression or localization of the heavy subunit of the Gal/GalNAc surface lectin. These results suggest no significant role of EhROM1 in complement resistance but unexpected roles in parasite adhesion and phagocytosis.

2

INTRODUCTION

Entamoeba histolytica is an extracellular protozoan parasite and is a leading parasitic cause of death worldwide (48). The factors, which determine the outcome of amebic infection, are currently unknown, although it is likely that a combination of host and parasite determinants influence clinical outcome. A number of parasite factors required for amebic pathogenesis have been identified including the Gal/GalNAc surface lectin, pore forming proteins and cysteine proteases (36-38, 41).

Recently, we identified several members of a class of intramembrane rhomboid proteases in the *E. histolytica* genome (4). Rhomboid proteases are seven-pass transmembrane proteases first identified in *Drosophila* whose active site lies within the lipid bilayer allowing them to cleave transmembrane proteins (6, 32). Substrates of rhomboid proteases are largely single pass transmembrane proteins whose transmembrane domain contains helix-breaking residues (52). Recent work has revealed that there are multiple classes of rhomboid proteases that recognize different types of sequences within the transmembrane domains of their substrates (3). Despite low sequence similarity between individual rhomboid proteases of each class, these enzymes share a remarkable ability to functionally replace one another (16, 28, 52).

Rhomboid proteases have been studied in flies, bacteria, mammals, and parasites and roles ranging from quorum sensing to host cell entry have been identified (3, 11, 25, 33, 35, 46, 47, 49, 54, 59). In Apicomplexan parasites such as *Plasmodium falciparum* and *Toxoplasma gondii*, it has been suggested that rhomboid proteases mediate cleavage of surface adhesin proteins to facilitate host cell entry (3, 11, 46, 47). The *E. histolytica* genome encodes four rhomboid-like genes, with only a single gene containing the necessary catalytic residues for proteolytic activity (4). This gene, EhROM1, is a functional protease with substrate specificity similar to the *P. falciparum* ROM4 (PfROM4) (3, 4). In trophozoites EhROM1 is localized to the parasite surface and relocalizes to internal vesicles during erythrophagocytosis and to the base of the

3

cap during surface receptor capping. We have shown that the heavy subunit of the amebic surface Gal/GalNAc lectin (Hgl) is a substrate of EhROM1 *in vitro*. Mutational analyses using a COS cell cleavage assay demonstrated that the cleavage of Hgl requires the catalytic serine in EhROM1 as well as a helix-breaking glycine residue in the transmembrane domain of Hgl (4). These data indicate that EhROM1 is a functional rhomboid protease whose physiological substrate may be Hgl.

In order to further elucidate the biological function of the EhROM1 we have utilized the epigenetic silencing mechanism of the *E. histolytica* G3 strain (8, 9). The mechanism of gene silencing in G3 ameba is not well understood. However, it is known that the silencing mechanism is epigenetically maintained and epigenetic changes in the chromatin state of the silenced genes have been noted (22). G3 parasites transfected with a plasmid containing an upstream region of the 5'end of EhROM showed almost complete downregulation of expression; we have named these parasites "ROM(KD)". Phenotypes we examined in ROM(KD) parasites included cap formation, complement resistance, adhesion, phagocytosis, hemolysis and motility. We observed defects in both adhesion and phagocytosis in the ROM(KD) parasites compared to the parent G3 strain but no changes in cap formation or complement resistance. Importantly, the reduced phagocytosis phenotype appears independent of the reduced adhesion phenotype, implicating that EhROM1 has distinct roles in both pathways.

MATERIALS AND METHODS

ROM silencing plasmid construction

In order to construct the silencing plasmid for EhROM1, the first 538 bp from the 5' end of *EhROM1* gene was cloned into the plasmid vector psAP-2 (8, 9) downstream to the 5'

4

upstream segment (473 bp) of the *EhAp-A* gene using a 5' NcoI site and a 3' BamHI site with the following primers: Forward: 5'-TACGCCATGGATTCTCCACCACATAAC-3', and Reverse: 5'-GCGGATCCCATCCCAAGTCTTAATTGCATTG-3' (restriction sites underlined in the primers).

Generation and maintenance of stable transfectants

G3 Parasites were transfected using two different methods (8, 9, 43). For the Superfect based method, trophozoites were seeded into 25 mm petri dishes and allowed to grow for 24 hr. On the day of transfection 20μg plasmid DNA was incubated for 10 min with 20μl Superfect (Qiagen) in a total volume of 200μl M199 media (Gibco). Cells were washed 1x with M199 followed by addition of 2ml M199 supplemented with 15% heat-inactivated bovine serum. The Superfect-DNA mixture was added in drops across the petri dish and the cells were covered by parafilm to minimize oxygen exposure. Parasites were incubated at 37°C for 4 hr, iced for 10 min to release parasites from the dish, and transferred to a 15ml glass tube containing fresh TYI medium. Parasites were allowed to grow for 48 hr after transfection before addition of drug selection. Parasites were selected at 1μg/ml Neomycin and increased to a final concentration of 2μg/ml G418. For the electroporation-based method, trophozoites were electroporated with 100μg plasmid DNA. Parasites were allowed to grow for 48 hrs before the addition of drug selection. Transfectants were selected at an initial concentration of 6μg/ml G418 (Geneticin). EhROM1 expression levels were tested using Northern blot analysis and reverse transcriptase PCR. Once EhROM1 downregulation was confirmed, the parasites were removed from drug selection, maintained under standard culture conditions, and tested monthly for maintenance of EhROM1 downregulation. All phenotypic analyses were done with parasite strains that had >95% decrease in EhROM1 expression levels and that were not under drug selection.

5

Northern blot analysis

Northern blot analysis was done as previously published (30). Briefly, total RNA was
isolated from parasites by phenol chloroform extraction, concentration determined using
a spectrophotometer and 20μg of each sample resolved on a gel containing 1 x MOPS,
1% agarose and 6% formaldehyde. RNA was transferred to Hybond N+ (Amersham)
nylon membrane, and crosslinked using UV light. The blots were pre-hybridized in
ExpressHyb (Clontech) hybridization buffer at 68°C for a minimum of 1 hr. Double
stranded PCR probes were labeled with ^{32}P-αdATP or ^{32}P-αdCTP using Klenow (New
England Biolabs) followed by hybridization of membranes at 68°C for approximately
18hr. Blots were washed as follows: the first wash for 25 min in buffer containing 2 x
SSC, 0.05% SDS, and the second wash in buffer containing 0.1 x SSC, 0.1% SDS.
Blots were then exposed overnight to a Kodak phosphor screen at room temperature.
Phosphor screens were scanned on a Biorad phosphor imager.

Reverse transcriptase PCR

Reverse transcriptase polymerase chain reaction (RT-PCR) was performed by
incubating approximately 2μg total RNA with DNAse for 15 min at 37°C. The reaction
was stopped by addition of EDTA to a concentration of 2.5mM followed by incubation at
65°C for 10 min. Following DNAse treatment, the RNA was separated into two aliquots.
One was kept on ice as a (–) RT control and the other was incubated with Superscript II
reverse transcriptase (Invitrogen) and 10mM dNTPs at 42°C for 2 hr. Remaining RNA
was hydrolyzed by addition of EDTA and NaOH and incubation at 70°C for 10 min.
Samples (both +/- RT) were diluted in 500μl TE buffer and passed through a YM-30

6

Microcon column (Millipore). 1µl cDNA was then used as a template for PCRs of EhROM1, Hgl, Lgl-1, or ssRNA. All PCRs were done for 35 cycles. Primers used were: EhROM1 (EHI_197460) F: 5'-AGGCCTTCATTCTCCACCACATAACAATA-3' and R: 5'-GAGCTCTTAATTGCATTTTCCAACATTG-3'; Hgl (EHI_077500) F: 5'-ACTAGTTTATAAACTTCACTTACC-3' and R: 5'-CCTAGGTCCATTGAATATTGCT-3'; Lgl-1 (EHI_035690) F: 5'-AGGCCTATGATTATATTAGTCTTATTGATA-3' and R: 5'-GAGCTCTTATGCAAACACAGGAATAA-3'; ssRNA (X61116) F: 5'-ACGAACGAGACTGAAACCTAT-3' and R: 5'- TGTTACGACTTCTCCTTCCTC-3'.

Complement resistance assays

To assay resistance of parasites to human complement, a previously published protocol was followed with some modifications (20). Briefly, trophozoites were harvested and washed in PBS and brought to a concentration of $1.2 – 1.5 \times 10^6$/ml. A total of 60,000-70,000 trophozoites were incubated with 10% normal human serum (NHS) in buffer containing: 1x PBS, 1.25 mM $MgCL_2$, 5mM EGTA for 20 or 40 min at 37°C. As a control for cell viability, trophozoites were incubated with 10% heat-inactivated NHS for 40 min. Parasites were then stained with 0.2% Trypan Blue in PBS followed by counting the total number of parasites and those which had excluded the dye. The average number of viable cells for the zero time point was set at 100% and each subsequent time point was calculated as a percentage of the initial time point.

Hemolysis assay

Hemolysis of HRBC by intact trophozoites was performed as previously described (34). In brief, *E. histolytica* trophozoites were mixed with HRBC at a ratio of 1:2000

7

trophozoites/HRBC (5×10^5 ameba:10^9 RBC) in 1ml of hemolysis buffer (100mM NaCl, 30mM KCl, 100mM sorbitol, 0.1% bovine serum albumin, and 10mM PIPES [piperazine-N,N9-bis(2-ethanesulfonic acid)]–Tris (pH 6.8)). The cell mixture was incubated for up to 90min at 37°C. The tubes were then spun down (1000g for 5min) and the hemoglobin that was released into the supernatant was read at 570 nm. The background used was HRBC incubated in the absence of trophozoites.

Transswell motility assays

Transwell motility assays were performed according to previous methods (17). Briefly, parasites were grown to confluence in T25 flasks. Adherent cells were washed once with serum-free TYI medium. The medium was then replaced with serum-free TYI supplemented with 2µg/ml CMFDA cell tracker dye (Invitrogen). Flasks were covered in foil and incubated at 37°C for 1 hr. After staining, parasites were removed from flasks using a cell scraper and quantified with a hemacytometer. Cells were pelleted and resuspended in serum-free TYI at a concentration of 500,000cells/ml and 300 µl of this mixture (150,000 parasites) was added to the top of each 24-well transwell insert containing 8µm pores (Co-star). One ml of complete TYI-S-33 medium was placed in the bottom of the chamber. A control well with no insert but an equivalent number of parasites in 1ml completed TYI media was used to normalize for potential differences in cell labeling. The 24-well plate was covered in foil, placed in an anaerobic bag for 4 hr at 37°C, after which the transwells were removed, media aspirated and replaced with 1ml of 1x PBS. Plates were read on a fluorescence plate reader at 492 nm (excitation) and 517 nm (emission).

8

Adherence assays

Adherence assays to healthy cells were performed using Chinese Hamster Ovary (CHO) cells according to previous methods (30). Briefly, approximately $1x10^4$ parasites plus $2x10^5$ CHO cells were mixed together in M199 (supplemented with 25mM HEPES pH6.8, 5.7mM Cysteine, 0.5% BSA, 10% HI bovine serum). This mixture was centrifuged at 150 x g for 5 min, and incubated on ice for 2 hr. After incubation, tubes were vortexed briefly and a hemocytometer was used to count parasites with CHO cells attached. Parasites with three or more cells attached were considered positive for adhesion. To test the effect of 3,4 dichloroisocoumarin (DCI) on parasite adhesion, 100μM DCI (Sigma-Aldrich) was dissolved in DMSO and applied to the parasites for 2 hours during the incubation. Control parasites were treated with DMSO alone.

Apoptotic CHO cells were generated using Staurosporine aglycone, an established inducer of apoptosis (5, 44). Prior to use, CHO cultures were enriched for viable cells by centrifugation at 600 rpm for 10min at RT by applying Ficoll-Paque PLUS (GE Healthcare). Viable cells were collected on top of the Ficoll-Paque layer and split into two groups. In one group apoptosis was induced by treatment with 100μM Staurosporine aglycone (Sigma-Aldrich) (dissolved in DMSO) for 1 h at 4˚C. Alternatively control parasites were treated with 100μM DMSO.

Induction of capping and Indirect Immunofluorescence assays

Capping was induced according to previous methods (1). Briefly, parasites were seeded into chamber slides (LabTek) and allowed to adhere at 37°C for 30 min. Parasites were rinsed once in 1xPBS (-CaCl₂). Then, 250μl 1xPBS with (20μg/ml), Concanavalin A (biotin labeled) was added to each chamber and parasites incubated on ice for 1 hr. After incubation on ice 750μl pre-warmed 1x PBS was added to each well, the wells covered with parafilm and slides placed in a 37°C water bath for 20 min to induce cap

9

formation. Buffer was subsequently removed and parasites fixed with 4% ultra-pure formaldehyde diluted in PBS + 10 mM $MgCl_2$ for 12 min. Cells were permeabilized by addition of 100% EtOH for 20 min followed by blocking in 3% BSA-PBS for 30 min. Cells were stained with primary antibody diluted in 1%BSA-PBS, incubated at RT for 1 hr, followed by staining with fluorescent secondary antibodies in the dark for 1 hr at RT. Antibody dilutions were as follows: Anti-Hgl (mouse monoclonal antibody) (3F4 and 7F4 together, each 1:30), anti-EhROM1 (rat polyclonal) (1:20), streptavidin Texas Red (1:500), Alexa 488 goat anti-mouse (1:1000), Alexa 488 goat anti-rat (1:1000). Imaging was performed on a Leica CTR6000 microscope, using a BD CARVII confocal unit. Image analysis and deconvolution was performed using the LAS-AF program from Leica. De-convolution was performed in ten iterations with a single de-convolved slice shown for each sample.

Phagocytosis assays

Erythrophagocytosis was performed as previously published (34). Briefly, 5×10^7 hRBCs were incubated with 5×10^5 trophozoites in 1ml PBS for 15 min at 37°C. The extracellular RBCs lysed by adding ice-cold distilled water and spinning the suspension twice. Pellets containing parasites and ingested hRBCs were lysed in concentrated formic acid (90%) and solutions read on a spectrophotometer at 397nm.

Ingestion of starch was assayed by microscopy. Trophozoites (1×10^5) were seeded into 12 well cell culture plates (Cellstar) and allowed to adhere for 2 h at 37°C. TYI-S-33 medium containing approximately 0.004% rice starch (MP Biomedicals) was added and incubated at 36.5°C for 1 hour. This was followed by PBS washes x3, fixation in 100% EtOH for 20 min, and staining with 1 % (v/v) Lugol's solution at RT for 5 min. Rice starch stained dark brown and parasites with one or more ingested starch

grains were considered positive for rice starch phagocytosis. A minimum of 100

parasites were counted for each treatment and the experiment was repeated a

minimum of 3 times.

Phagocytosis of CHO cells was performed as follows. Prior to use, CHO cultures

were enriched for viable cells by applying Ficoll-Paque PLUS method as previously

outlined. 0.5×10^5 CHO cells were treated with apoptosis-inducing condition (100 μM

Staurosporine) or as control (100 μM DMSO) for 1 h at 4°C and added to parasites (1:1

ratio) by spinning at 200 rpm for 5 min. Parasite-CHO cells were incubated for 15 min at

36.5 °C, fixed with 4% formaldehyde for 12 min, permeabilized in 100% EtOH for 20 min

and stained with 1% (v/v) Trichrome stain. Parasites with one or more ingested CHO

cell were considered positive for phagocytosis. A minimum of 50 parasites were

counted for each treatment and the experiment was repeated a minimum of 3 times.

Western blot analysis

Lysates were prepared using log phase trophozoites. Trophozoites were iced for 10

min, pelleted at 1000 x g for 5 min at 4°C followed by a single wash in ice cold 1x PBS.

Parasites were resuspended in lysis buffer (50mM HEPES-KOH pH7.5, 50mM KCl,

5mM $MgCl_2$, 0.5% NP-40) containing protease inhibitors (2mM DTT, 375μM E-64,

0.4μg/ml Leupeptin, 1x HALT inhibitor cocktail (#78410 Thermo Scientific)), incubated

on ice and a Bradford assay used to determine protein concentration. Lysates were run

on a standard 8-10%SDS-PAGE gel and transferred overnight at 35 mAmp at 4°C to

PVDF membrane. The membrane was blocked with 5% milk in PBS-0.1% Tween-20 for

a minimum of 1 hr. Blots were then incubated with antibodies to Hgl (H85, 1:50), Pan

Actin (Cell Signaling) (1:250), or α-EhROM1 (1:1000), diluted in 5% milk, PBS-0.1%

Tween-20 overnight at 4°C followed by incubation with secondary HRP-conjugated

11

antibodies diluted in the same solution (1:1000 or 1:5000) and developed using ECL. Blots were scanned on a Kodak Image Station 4000R.

E. histolytica Gal/GalNAc lectin ELISA

For quantification of *E. histolytica* lectin present in the whole amebic cell lysates as well as in conditioned TYI-S-33 serum-free media *E. histolytica* II lectin enzyme immunoassay (Techlab) was performed according to the manufactures instructions. Briefly, amebic lysates were prepared as described for Western blot and adjusted to 50ng of total protein. Conditioned media was prepared by growing log-phase trophozoites in serum-free media for 24 h. Media was collected and centrifuged 1000 x g for 5 min at 4°C to pellet intact amebas and further subjected to ultra-centrifugation at 210,000 x g for 30 min at 4°C. Prior to use the total media protein concentration was adjusted to 400 ng. The microassay plate was coated with monoclonal antibody specific for *E. histolytica* lectin and incubated directly with a sample. An internal sample of purified *E. histolytica* lectin was used as a positive control and assay diluent as negative control. After washing 5 times, the ELISA was developed by adding the substrate to the plate followed by the stop solution. The amebic lectin was quantified by measuring the optical density at 450nm on a microplate ELISA reader. The experiment was performed 3 times and results averaged.

Microarray analysis of ROM(KD) parasites

To identify potential changes in gene expression of the Gal/GalNAc lectin due to ROM1 silencing, total RNA from G3 or ROM(KD) parasites was isolated with Trizol reagent (Invitrogen) using standard protocols (29). The RNA samples were further cleaned with the RNeasy kit (Qiagen) before being used for microarray analysis. Samples were processed for microarray hybridization by the Stanford University Protein and Nucleic

12

Acids facility (http://cmgm.stanford.edu/pan/) using standard protocols. For each sample the RNA quality was checked using an Agilent BioAnalyser QC. RNA samples (4 mg) were labeled and hybridized to a custom Affymetrix array full genome microarray (18) using standard protocols. Raw probe intensities generated by the GCOS software (http:// www.affymetrix.com/products/software/specific/gcos.affx) were processed in R 2.2.0 using robust multiarray averaging with correction for oligo sequence (gcRMA), downloaded from the BioConductor project (http://www.bioconductor.org). Two independent biological samples of G3 and ROM(KD) parasites were analyzed. Genes annotated as Gal/GalNAc lectin (heavy and light subunit) and rhomboid protease (EhROM1-4) were analyzed for expression levels. A control gene, Actin (EHI_163580) was also analyzed. Results of the microarray were confirmed by semi-quantitative RT-PCR using methods outlined above.

RESULTS

Downregulation of EhROM1 in *E. histolytica* G3 strain

In order to elucidate the function of EhROM1 we sought to downregulate its expression. We utilized a number of approaches including dsRNA expression, inducible expression of antisense transcript, and constitutive expression of antisense transcript but were unable to significantly downregulate expression of EhROM1 using any of these methods (data not shown). We also generated an EhROM1 S-A catalytic mutant, which may function in a dominant negative fashion. However, this construct did not target appropriately to the parasite surface (data not shown). In our experience both N and C-terminally tagged EhROM1 fusion proteins did not localize to the parasite surface, regardless of the use of a small (Myc) or large (GFP) tag (data not shown). Therefore,

13

any phenotype due to presence of EhROM1 on the parasite surface would be difficult to assess using a tagged EhROM1 S-A catalytic mutant.

Thus, we chose to use the epigenetic silencing mechanism utilizing the *E. histolytica* G3 line of parasites (8, 9, 12). We utilized a plasmid containing the *EhAp-A* 5' upstream region cloned upstream of the first 538 bp from the 5' end of *EhROM1* (Fig. 1A). We generated stable transfectants in drug selection for approximately one month and examined expression of EhROM1. Two independent lines of transfectants with downregulation of EhROM1 were generated; one line was generated by electroporation in the Mirelman lab and another line was generated by lipid-based transfection in the Singh lab. Transfectants from both labs were maintained in drug selection for at least one month prior to removal of drug selection. Parasites were cured of plasmid in order to avoid any secondary phenotypic effects caused by drug selection. Transfectants in the Mirelman lab were cloned from a single parasite while those in the Singh lab were maintained as a heterogeneous population. Both lines of parasites were assayed by Northern blot, RT-PCR and Western blot for expression of EhROM1 transcript and protein respectively. For both transfectant parasite lines, expression of EhROM1 transcript was undetectable by Northern blot (Fig. 1B), while RT-PCR revealed a small amount (<5%) of EhROM1 transcript present (Fig. 1C). Western blots revealed no signal from an EhROM1-specific antibody (Fig. 1D). Thus both lines of transfectants were named "ROM(KD)" as they exhibited greater than 95% knockdown of EhROM1 expression at the RNA and protein level. Representative data from transfectants in the Mirelman lab (Fig. 1D) and Singh lab (Fig. 1B, 1C) are shown. Additionally our microarray data confirmed the down regulation of EhROM1 expression by 479-fold in ROM(KD) parasites compared to G3 (Fig. 5A). Expression levels of other ROMs were not significantly changed.

14

ROM(KD) parasites are not altered in cap formation

Our previous data indicate that the heavy subunit of the Gal/GalNAc lectin, Hgl, is a substrate of EhROM1 *in vitro* (4). In order to study the biological function of potential Hgl cleavage by EhROM1 in trophozoites we selected a wide range of phenotypic assays to examine in ROM(KD) parasites. Phenotypes examined included: surface receptor capping, localization of Hgl to caps, complement resistance, adhesion, phagocytosis and motility. For all assays we compared ROM(KD) parasites removed from Neomycin selection to G3 parasites in order to avoid any secondary effects of drug selection.

E. histolytica employs a number of strategies to avoid lysis by the host complement system (13, 15, 21, 39, 40, 45). Surface receptor capping is one mechanism that is induced by the presence of antibodies directed against parasite surface proteins. Binding of antibodies to surface receptors on the parasite results in the polarization of these receptors to the posterior end where they form a cap (13, 14, 45). The cap is subsequently released from the parasite (through an unknown mechanism) allowing the parasite to evade the host immune system. Other mechanisms of complement resistance in *E. histolytica* include cleavage of components of the membrane attack complex by parasite proteases and homology between human CD-59 and the heavy subunit of the amebic lectin, which prevents assembly of the membrane attack complex on the parasite surface (10, 39, 40). We have shown previously that EhROM1 relocalizes to the base of the caps formed during surface receptor capping (4). The amebic Gal/GalNAc lectin is known to elicit a robust antibody response in the host and is thus one of the proteins targeted to the cap for release (13-15). Our previous work identified the heavy subunit of this lectin as a substrate of EhROM1 *in vitro* (4). In order to determine whether the relocalization of EhROM1 to the base of the cap indicates that it plays a role in cap formation, release, or cleavage of Hgl we examined

15

cap formation, localization of Hgl to the cap, and complement resistance in ROM(KD) parasites.

Capping was induced *in vitro* by incubating parasites with a synthetic lectin, Concanavalin A (ConA), followed by incubating parasites at 37°C for 15 min. Parasites were fixed and stained to allow visualization of the ConA (which has a biotin tag) and either Hgl or EhROM1. We observed the formation of morphologically indistinguishable caps in both G3 and ROM(KD) parasites (Fig. 2A, 2B). ROM(KD) parasites showed low signal with the EhROM1 antibody, as expected (Fig. 2A). Caps in both ROM(KD) and G3 parasites showed dramatic enrichment of Hgl (Fig. 2B).

ROM(KD) parasites display no change in complement resistance or motility
In order to examine a biologically relevant phenotype associated with capping we examined the ability of ROM(KD) parasites to resist lysis by human complement. Complement resistance was measured by incubating G3 or ROM(KD) parasites with human serum for 20 or 40 min followed by Trypan blue staining to assess parasite viability. No change in complement resistance was observed in ROM(KD) parasites compared to G3 (Fig. 3A). Between 60-70% of parasites were killed after a 20 min incubation with serum and between 70-80% were killed after 40 min. These data indicate that ROM(KD) parasites exhibit no change in cap formation or complement resistance.

Parasite motility is a key virulence factor as it is required for multiple steps of the invasion process (27, 57). Parasites must maneuver across the colonic epithelium, penetrate the destroyed epithelial barrier and travel to extraintestinal sites of infection. Due to the localization of EhROM1 to the parasite surface and the potential for this protease to cleave surface adhesins we decided to investigate any changes in amebic

16

motility associated with downregulation of EhROM1 expression. A transwell assay has been developed to measure motility in *E. histolytica* (17). Parasites are labeled with a fluorescent cell tracking dye CMFDA and placed in the top chamber of a transwell system resuspended in serum-free media. The bottom chamber below the transwell is filled with serum-containing media in order to induce parasite migration from the upper chamber to the lower chamber. Pores in the transwell are smaller than parasites and thus require parasites to use active motility to migrate through these pores. We performed transwell motility assays in parallel for G3 and ROM(KD) parasites and observed no change in transwell migration between these parasite lines (Fig. 3B). Despite many studies demonstrating their cleavage of parasite surface adhesins, rhomboid proteases have not been implicated in parasite motility (3, 11, 47). Disruption of *P. berghei* ROM1 did not affect sporozoite gliding motility suggesting that surface proteins involved in this type of motility are not rhomboid substrates (47).

ROM(KD) parasites have an adherence defect to healthy host cells

Adhesion to host cells is a crucial step in the pathogenesis of *E. histolytica*. Binding of the parasite Gal/GalNAc lectin to host cells is a required step for the induction of apoptosis in host cells and cytotoxicity (24, 36, 42). We have shown previously that EhROM1 is localized to the surface of trophozoites; thus it could potentially play a role in regulating parasite adhesion (4). In order to investigate this possibility we measured the ability of both G3 and ROM(KD) parasites to adhere to healthy (untreated) CHO cells using a standard CHO cell rosette assay (30). Adhesion assays comparing G3 and ROM(KD) parasites showed a consistent ~35% decrease in adhesion by ROM(KD) compared to G3 parasites (p<0.001)(Fig. 4A).

17

In order to corroborate the adhesion phenotype with another assay in which EhROM1 is inhibited, we examined the effect of rhomboid protease inhibitors on parasite adhesion to host cells. It has been demonstrated that isocoumarin compounds including 3,4 dichloroisocoumarin (DCI) inhibit rhomboid proteases by alkylating the histidine, whereas compounds directed against the serine nucleophile (such as phenylmethylsulfonyl fluoride (PMSF)) did not have any significant effect on substrate cleavage by rhomboid proteases (55). We tested the effect of DCI on *E. histolytica* HM-1:IMSS trophozoites and identified that in the presence of 100 μM DCI, parasites had a ~60% decrease in adhesion compared to controls (DMSO or PMSF) (Fig. 4B). These results were achieved with the wild-type *E. histolytica* HM-1:IMSS strain but also recapitulated with the G3 strain (data not shown). Since DCI, an inhibitor of rhomboid proteases recapitulates the ROM(KD) adhesion defect (in both wild-type HM-1:IMSS and G3 strains), we propose that these data are consistent with a role in parasite adhesion for EhROM1. However, since DCI may have other unknown effects on *E. histolytica* trophozoites, the ROM(KD) strain is still the best way to specifically assess the function of EhROM1 in amebic trophozoites.

No significant changes in RNA or protein levels of Gal/GalNAc lectin are noted in the ROM(KD) parasites

The Gal/GalNAc lectin is one of the primary receptors known to be involved in mediating trophozoite adhesion (38, 42). In order to better understand the adhesion defect of ROM(KD) parasites, we investigated whether there were any potential changes in expression or subcellular localization of Hgl. We observed no alterations in expression levels of the heavy subunit of the Gal/GalNAc lectin by microarray analysis (Fig. 5A), RT-PCR (Fig. 5B), Western blot (Fig. 6A) or ELISA (Fig. 6B and 6C). All techniques revealed that there was no major change in expression or protein level of either Hgl or

18

Lgl-1 in ROM(KD) compared to G3 parasites. Additionally no significant changes of lectin levels in amebic lysates or in conditioned media were noted as measured by an Hgl ELISA (Fig. 6C). We next examined whether any changes in the subcellular localization of Hgl could explain the defect we observed in adhesion of ROM(KD) parasites to CHO cells. Immunofluorescence imaging revealed no dramatic difference in surface or internal Hgl localization between G3 and ROM(KD) parasites in permeabilized and non-permeabilized samples respectively (Fig. 6D). Taken together, the adhesion defect of ROM(KD) parasites cannot be attributed to any changes in expression or localization of the amebic surface lectin.

ROM(KD) parasites have decreased phagocytic ability compared to G3 parasites

Erythrophagocytosis is one indicator of amebic virulence potential. Pathogenic *E. histolytica* ingests erythrocytes while nonpathogenic species such as *E. dispar* do not -- a difference which has historically been used to diagnose which species of *Entamoeba* an individual was infected with (51). Attachment to erythrocytes has been shown to be mediated by both the amebic Gal/GalNAc lectin as well as a transmembrane kinase (7, 36, 56). We have previously shown that EhROM1 localizes to phagocytic vesicles during erythrophagocytosis, suggesting that it could play a role in this process. We measured erythrophagocytosis in G3 and ROM(KD) parasites using a colorimetric assay; parasites are incubated with erythrocytes, extracellular erythrocytes are lysed in distilled water and parasites containing ingested erythrocytes are lysed in concentrated formic acid. The resulting solution is measured with a spectrophotometer in order to quantify ingested erythrocytes. We compared the ability of G3 and ROM(KD) parasites to ingest human erythrocytes and observed a defect in erythrophagocytosis in ROM(KD) parasites compared to G3 (p<0.001) (Fig. 7A). In both G3 and ROM(KD) parasites the addition of galactose (but not glucose) significantly inhibited (>60%) the

19

rates of erythrophagocytosis, which confirms the role of the Gal/GalNAc lectin in erythrophagocytosis in these parasite strains (data not shown). It is noteworthy that no difference was detected in the hemolytic activity between G3 and ROM(KD) trophozoites (data not shown).

In order to investigate the role of EhROM1 during phagocytosis of another substrate, we compared the ability of ROM(KD) and G3 parasites to ingest the rice starch. We considered parasites that had ingested at least one starch grain as actively phagocytic. Phagocytosis of rice starch was decreased by 25% in ROM(KD) compared to G3 ($p<0.006$) (Fig. 7B). Thus, ROM(KD) parasites have a general decrease in their phagocytic ability.

ROM(KD) parasites have normal adherence to but decreased phagocytosis of apoptotic cells

There appear to be distinct receptors for amebic adhesion to healthy and apoptotic cells. The Gal/GalNAc lectin is involved in adhesion to healthy cells (38, 42). The phagosome-associated transmembrane kinase (PATMK) was shown to play a role in adhesion to both healthy and dying erythrocytes (7). Additionally, an immunogenic surface protein, the serine-rich *E. histolytica* protein (SREHP) identified in a screen for antibodies that blocked adhesion of trophozoites to apoptotic cells was shown to be the major receptor utilized by parasites during adhesion to apoptotic cells (50). Therefore, assaying the ability of ROM(KD) parasites to adhere to both healthy and apoptotic cells would help to further define whether the adhesion defect of ROM(KD) was due solely to the Gal/GalNAc lectin alone.

20

In order to determine whether ROM(KD) parasites had differential adherence to healthy and apoptotic cells, we measured adherence to healthy and Staurosporine-treated cells. Staurosporine treatment consistently resulted in greater than 70-85% apoptotic cells, as determined by the presence of phosphatidylserine on the outer leaflet of the CHO cell plasma membrane measured by the BD Pharmingen Annexin V-FITC Fluorescence Microscopy Kit (data not shown). The adherence of G3 parasites to Staurosporine-treated CHO cells was significantly diminished compared to DMSO treated CHO cells ($p<0.002$). This is consistent with previous studies which demonstrate decreased adherence of apoptotic cells to amebic trophozoites (23). ROM(KD) parasites incubated with DMSO-treated CHO cells had a consistent ~25% decrease in adhesion compared to G3 parasites (Fig.8A), similar to the adhesion defect of ROM(KD) to healthy non-treated CHO cells (Fig. 4A) The adherence of ROM(KD) parasites to Staurosporine-treated CHO cells was less affected and was comparable to the G3 parasite (though significantly decreased compared to DMSO controls (p-value< 0.003))(Fig. 8A).

Next we assessed the ability of G3 and ROM(KD) parasites to phagocytose apoptotic CHO cells. It has previously been reported that phosphatidylserine exposure (as occurs in apoptotic cells) enhances *E. histolytica* engulfment of host cells (2, 23). We observed a similar phenomenon; G3 parasites had relatively increased ingestion of apoptotic cells compared to control (DMSO-treated) cells, once its reduced adherence defect is taken into account (Fig. 8A and 8B). However, ROM(KD) parasites had significantly reduced phagocytosis of apoptotic cells, despite adhering to apoptotic cells at levels comparable to G3 parasites (Fig. 8B) ($p<0.007$). These data implicate that ROM(KD) parasites have two independent phenotypes: decreased adherence and decreased phagocytosis.

21

DISCUSSION

We downregulated expression of EhROM1 utilizing the epigenetic method in *E. histolytica* G3 parasites (8, 9, 12). Phenotypes associated with amebic pathogenesis were examined in these parasites. These assays were selected based on the premise that Hgl, the heavy subunit of the Gal/GalNAc lectin and a major virulence determinant in *E. histolytica*, may be a substrate of EhROM1 (4). Additionally, phenotypes were analyzed based on presence of EhROM1 on the parasite surface and relocalization of EhROM1 to internal vesicles during erythrophagocytosis and to the base of caps during surface receptor capping (4). We demonstrated that ROM(KD) parasites had defects in adhesion to healthy cells, whereas adhesion to apoptotic cells was comparable to levels seen in the parent G3 strain. A generalized phagocytosis defect was noted in ROM(KD) parasites, with reduced phagocytosis of erythrocytes and rice starch. Additionally, despite adhering to apoptotic cells at levels comparable to the G3 strain, ROM(KD) parasites had decreased phagocytosis of apoptotic cells. Taken together, the data indicate that the reduced adhesion and phagocytosis phenotypes of ROM(KD) parasites are two independent features of EhROM1. Whether these two phenotypes are mediated through one or two distinct EhROM1 target(s) is not known. We have previously demonstrated that the heavy subunit of the Gal/GalNAc lectin is a target for EhROM1, but additional targets could also be present. Rhomboid proteases have been implicated in development, signaling, apoptosis, and host cell entry (3, 11, 49, 53, 58, 60). Thus roles in adhesion and phagocytosis would both be new functions for rhomboid proteases. Our data represent the first study of a rhomboid protease in an extracellular parasitic pathogen and broaden the potential functional roles played by rhomboid proteases across evolution (16).

The adhesion defect observed in ROM(KD) parasites was unexpected since we hypothesized that EhROM1 could cleave the Gal/GalNAc lectin, which mediates

22

parasite adhesion to host cells. Thus, EhROM1 downregulation would be postulated to increase surface abundance of the Gal/GalNAc lectin, and thus increase parasite adhesion. Interestingly, there were no significant changes in expression or localization of the heavy subunit of the Gal/GalNAc lectin in ROM(KD) parasites. Multiple models can explain the unexpected result of ROM(KD) parasites being less adherent. One possibility is that EhROM1 cleaves a substrate on the host cell surface, which requires processing for adhesion. In this scenario EhROM1 would more likely cleave a juxtamembrane site of the host cell surface protein as it is unlikely that EhROM1 would be able to cleave within the transmembrane domain. Rhomboid proteases have recently been shown to be able to cleave regions outside the transmembrane domain so this possibility is feasible (19, 31). A second possibility is that EhROM1 may cleave an unknown substrate on the parasite surface, which masks the Gal/GalNAc lectin under normal conditions. Thus, cleavage and shedding of this surface protein is required in order for the Gal/GalNAc lectin to be accessible to host cells. A third model is that EhROM1, rather than modulating direct attachment between the parasite and host cell, has a role in signaling during the adhesion process. The cytoplasmic domain of Gal/GalNAc lectin contains a β-integrin-like motif, which regulates signaling and plays a role in both adherence and virulence (56). EhROM1-mediated cleavage of the lectin would inhibit inside-out signaling from this domain by severing the attachment between the extracellular and intracellular portions of Hgl. Finally, it is possible that EhROM1 has a non-catalytic role in the adhesion process as non-catalytic functions of rhomboid proteases have been described (26).

ROM(KD) parasites exhibited no alteration in cap formation or complement resistance compared to G3 parasites. One explanation for this is that the small amount of EhROM1 still present in ROM(KD) parasites is able to functionally compensate for these biological processes. Previous biochemical analyses have shown that EhROM1 is

a highly active protease (4), so it is possible that despite the very significant downregulation of EhROM1, enough functional protease is still present. Additionally, *E. histolytica* has multiple other means by which it evades the complement cascade including degradation of components of the membrane attack complex (MAC) by amebic proteases as well as the homology between Hgl and human CD-59 which prevents assembly of the MAC on the cell surface (10, 39, 40). Thus, a defect in complement resistance could be masked by compensatory changes in these other mechanisms, which should still be fully functional in ROM(KD) parasites. One final consideration is that the relocalization of EhROM1 to the base of the cap is a passive event. Thus, EhROM1 is excluded from the cap because of its multi-pass transmembrane architecture and that it does not play significant roles in capping or complement resistance. According to the latest available genome data, *E. histolytica* encodes a single rhomboid protease with the residues required for proteolytic activity. Thus, to the best of our knowledge, no other rhomboid protease exists which could compensate for the loss-of-function in ROM(KD) parasites. Relocalization of EhROM1 to the base of the cap was most dramatic when the cap appeared to pinch off for release (4). Further approaches (using live imaging for example) to study the process of cap release process would provide invaluable data as to whether EhROM1 plays a role in this process.

Our data suggest two distinct roles of EhROM1: in regulating parasite adhesion to viable (but not to apoptotic) host cells and in phagocytosis. The underlying mechanism behind defects in adhesion and phagocytosis in ROM(KD) parasites are unclear and will require further investigation. In order to further elucidate the role of EhROM1, expression of this gene should be downregulated in a virulent parasite strain in order to examine phenotypes that could not be measured in G3 parasites. Additionally, whether the Gal/GalNAc lectin is cleaved by EhROM1 in parasites or

24

whether other substrates of EhROM1 exist are important future avenues of investigation.

25

REFERENCES

1.   **Arhets, P., P. Gounon, P. Sansonetti, and N. Guillen**. 1995. Myosin II is involved in capping and uroid formation in the human pathogen *Entamoeba histolytica*. Infect Immun **63**:4358-4367.

2.   **Bailey, G. B., D. B. Day, C. Nokkaew, and C. C. Harper**. 1987. Stimulation by target cell membrane lipid of actin polymerization and phagocytosis by *Entamoeba histolytica*. Infect Immun **55**:1848-1853.

3.   **Baker, R. P., R. Wijetilaka, and S. Urban**. 2006. Two *Plasmodium* rhomboid proteases preferentially cleave different adhesins implicated in all invasive stages of malaria. PLoS Pathog **2**:e113.

4.   **Baxt, L. A., R. P. Baker, U. Singh, and S. Urban**. 2008. An *Entamoeba histolytica* rhomboid protease with atypical specificity cleaves a surface lectin involved in phagocytosis and immune evasion. Genes Dev **22**:1636-1646.

5.   **Belmokhtar, C. A., J. Hillion, and E. Segal-Bendirdjian**. 2001. Staurosporine induces apoptosis through both caspase-dependent and caspase-independent mechanisms. Oncogene **20**:3354-3362.

6.   **Bier, E., L. Y. Jan, and Y. N. Jan**. 1990. rhomboid, a gene required for dorsoventral axis establishment and peripheral nervous system development in *Drosophila melanogaster.* Genes Dev **4**:190-203.

7.   **Boettner, D. R., C. D. Huston, A. S. Linford, S. N. Buss, E. Houpt, N. E. Sherman, and W. A. Petri, Jr.** 2008. *Entamoeba histolytica* phagocytosis of human erythrocytes involves PATMK, a member of the transmembrane kinase family. PLoS Pathog **4**:e8.

8.   **Bracha, R., Y. Nuchamowitz, M. Anbar, and D. Mirelman**. 2006. Transcriptional silencing of multiple genes in trophozoites of *Entamoeba histolytica*. PLoS Pathog **2**:e48.

26

9. **Bracha, R., Y. Nuchamowitz, and D. Mirelman**. 2003. Transcriptional silencing of an amoebapore gene in *Entamoeba histolytica*: molecular analysis and effect on pathogenicity. Eukaryot Cell **2**:295-305.

10. **Braga, L. L., H. Ninomiya, J. J. McCoy, K. Adal, T. Wiedmer, C. Pham, P. J. Sims, and W. A. Petri, Jr.** 1992. Inhibition of the complement membrane attack complex by the galactose-specific adhesin of *Entamoeba histolytica*. Arch Med Res **23**:133.

11. **Brossier, F., T. J. Jewett, L. D. Sibley, and S. Urban**. 2005. A spatially localized rhomboid protease cleaves cell surface adhesins essential for invasion by *Toxoplasma*. Proc Natl Acad Sci U S A **102**:4146-4151.

12. **Bujanover, S., U. Katz, R. Bracha, and D. Mirelman**. 2003. A virulence attenuated amoebapore-less mutant of *Entamoeba histolytica* and its interaction with host cells. Int J Parasitol **33**:1655-1663.

13. **Calderon, J.** 1980. Dynamic changes on the surface of Entamoeba induced by antibodies. Arch Invest Med (Mex) **11**:55-61.

14. **Calderon, J., and E. E. Avila**. 1986. Antibody-induced caps in *Entamoeba histolytica*: isolation and electrophoretic analysis. J Infect Dis **153**:927-932.

15. **Espinosa-Cantellano, M., and A. Martinez-Palomo**. 1994. *Entamoeba histolytica*: mechanism of surface receptor capping. Exp Parasitol **79**:424-435.

16. **Freeman, M.** 2009. Rhomboids: 7 years of a new protease family. Semin Cell Dev Biol **20**:231-239.

17. **Gilchrist, C. A., D. J. Baba, Y. Zhang, O. Crasta, C. Evans, E. Caler, B. W. Sobral, C. B. Bousquet, M. Leo, A. Hochreiter, S. K. Connell, B. J. Mann, and W. A. Petri**. 2008. Targets of the *Entamoeba histolytica* Transcription Factor URE3-BP. PLoS Negl Trop Dis **2**:e282.

18. **Gilchrist, C. A., E. Houpt, N. Trapaidze, Z. Fei, O. Crasta, A. Asgharpour, C. Evans, S. Martino-Catt, D. J. Baba, S. Stroup, S. Hamano, G. Ehrenkaufer, M.**

27

Okada, U. Singh, T. Nozaki, B. J. Mann, and W. A. Petri, Jr. 2006. Impact of intestinal colonization and invasion on the *Entamoeba histolytic*a transcriptome. Mol Biochem Parasitol **147**:163-176.

19.   **Ha, Y.** 2009. Structure and mechanism of intramembrane protease. Semin Cell Dev Biol **20**:240-250.

20.   **Hamelmann, C., B. Foerster, G. D. Burchard, N. Shetty, and R. D. Horstmann**. 1993. Induction of complement resistance in cloned pathogenic *Entamoeba histolytica*. Parasite Immunol **15**:223-228.

21.   **Hamelmann, C., B. Urban, B. Foerster, and R. D. Horstmann**. 1993. Complement resistance of pathogenic *Entamoeba histolytica* mediated by trypsin-sensitive surface component(s). Infect Immun **61**:1636-1640.

22.   **Huguenin, M., R. Bracha, T. Chookajorn, and D. Mirelman**. 2009. Epigenetic transcriptional gene silencing in *Entamoeba histolytica*: insight into histone and chromatin modifications. Parasitology:1-9.

23.   **Huston, C. D., D. R. Boettner, V. Miller-Sims, and W. A. Petri, Jr.** 2003. Apoptotic killing and phagocytosis of host cells by the parasite *Entamoeba histolytica*. Infect Immun **71**:964-972.

24.   **Huston, C. D., E. R. Houpt, B. J. Mann, C. S. Hahn, and W. A. Petri, Jr.** 2000. Caspase 3-dependent killing of host cells by the parasite *Entamoeba histolytica*. Cell Microbiol **2**:617-625.

25.   **Kanaoka, M. M., S. Urban, M. Freeman, and K. Okada**. 2005. An *Arabidopsis* Rhomboid homolog is an intramembrane protease in plants. FEBS Lett **579**:5723-5728.

26.   **Karakasis, K., D. Taylor, and K. Ko**. 2007. Uncovering a link between a plastid translocon component and rhomboid proteases using yeast mitochondria-based assays. Plant Cell Physiol **48**:655-661.

27.   **Labruyere, E., and N. Guillen**. 2006. Host tissue invasion by *Entamoeba histolytica* is powered by motility and phagocytosis. Arch Med Res **37**:253-258.

28

28.   **Lemberg, M. K., and M. Freeman**. 2007. Cutting proteins within lipid bilayers: rhomboid structure and mechanism. Mol Cell **28**:930-940.

29.   **MacFarlane, R. C., and U. Singh**. 2006. Identification of differentially expressed genes in virulent and nonvirulent *Entamoeba* species: potential implications for amebic pathogenesis. Infect Immun **74**:340-351.

30.   **MacFarlane, R. C., and U. Singh**. 2007. Identification of an *Entamoeba histolytica* serine-, threonine-, and isoleucine-rich protein with roles in adhesion and cytotoxicity. Eukaryot Cell **6**:2139-2146.

31.   **Maegawa, S., K. Koide, K. Ito, and Y. Akiyama**. 2007. The intramembrane active site of GlpG, an *E. coli* rhomboid protease, is accessible to water and hydrolyses an extramembrane peptide bond of substrates. Mol Microbiol **64**:435-447.

32.   **Mayer, U., and C. Nusslein-Volhard**. 1988. A group of genes required for pattern formation in the ventral ectoderm of the *Drosophila* embryo. Genes Dev **2**:1496-1511.

33.   **McQuibban, G. A., S. Saurya, and M. Freeman**. 2003. Mitochondrial membrane remodelling regulated by a conserved rhomboid protease. Nature **423**:537-541.

34.   **Mora-Galindo, J., M. Gutierrez-Lozano, and F. Anaya-Velazquez**. 1997. *Entamoeba histolytica*: kinetics of hemolytic activity, erythrophagocytosis and digestion of erythrocytes. Arch Med Res **28 Spec No**:200-201.

35.   **Pascall, J. C., and K. D. Brown**. 2004. Intramembrane cleavage of ephrinB3 by the human rhomboid family protease, RHBDL2. Biochem Biophys Res Commun **317**:244-252.

36.   **Petri, W. A., Jr., R. D. Smith, P. H. Schlesinger, C. F. Murphy, and J. I. Ravdin**. 1987. Isolation of the galactose-binding lectin that mediates the in vitro adherence of *Entamoeba histolytica*. J Clin Invest **80**:1238-1244.

37.   **Que, X., and S. L. Reed**. 1997. The role of extracellular cysteine proteinases in pathogenesis of *Entamoeba histolytica* invasion. Parasitol Today **13**:190-194.

29

38. **Ravdin, J. I., C. F. Murphy, R. A. Salata, R. L. Guerrant, and E. L. Hewlett**. 1985. N-Acetyl-D-galactosamine-inhibitable adherence lectin of *Entamoeba histolytica*. I. Partial purification and relation to amoebic virulence in vitro. J Infect Dis **151**:804-815.

39. **Reed, S. L., J. A. Ember, D. S. Herdman, R. G. DiScipio, T. E. Hugli, and I. Gigli**. 1995. The extracellular neutral cysteine proteinase of *Entamoeba histolytica* degrades anaphylatoxins C3a and C5a. J Immunol **155**:266-274.

40. **Reed, S. L., W. E. Keene, J. H. McKerrow, and I. Gigli**. 1989. Cleavage of C3 by a neutral cysteine proteinase of *Entamoeba histolytica*. J Immunol **143**:189-195.

41. **Rosenberg, I., D. Bach, L. M. Loew, and C. Gitler**. 1989. Isolation, characterization and partial purification of a transferable membrane channel (amoebapore) produced by *Entamoeba histolytica*. Mol Biochem Parasitol **33**:237-247.

42. **Saffer, L. D., and W. A. Petri, Jr.** 1991. Role of the galactose lectin of *Entamoeba histolytica* in adherence-dependent killing of mammalian cells. Infect Immun **59**:4681-4683.

43. **Saito-Nakano, Y., T. Yasuda, K. Nakada-Tsukui, M. Leippe, and T. Nozaki**. 2004. Rab5-associated vacuoles play a unique role in phagocytosis of the enteric protozoan parasite *Entamoeba histolytica*. J Biol Chem **279**:49497-49507.

44. **Segal-Bendirdjian, E., and A. Jacquemin-Sablon**. 1995. Cisplatin resistance in a murine leukemia cell line is associated with a defective apoptotic process. Exp Cell Res **218**:201-212.

45. **Silva, P. P., A. Martinez-Palomo, and A. Gonzalez-Robles**. 1975. Membrane structure and surface coat of *Entamoeba histolytica*. Topochemistry and dynamics of the cell surface: cap formation and microexudate. J Cell Biol **64**:538-550.

46. **Singh, S., M. Plassmeyer, D. Gaur, and L. H. Miller**. 2007. Mononeme: a new secretory organelle in *Plasmodium falciparum* merozoites identified by localization of rhomboid-1 protease. Proc Natl Acad Sci U S A **104**:20043-20048.

30

47.   **Srinivasan, P., I. Coppens, and M. Jacobs-Lorena**. 2009. Distinct roles of *Plasmodium* rhomboid 1 in parasite development and malaria pathogenesis. PLoS Pathog **5**:e1000262.

48.   **Stauffer, W., and J. I. Ravdin**. 2003. *Entamoeba histolytica*: an update. Curr Opin Infect Dis **16**:479-485.

49.   **Stevenson, L. G., K. Strisovsky, K. M. Clemmer, S. Bhatt, M. Freeman, and P. N. Rather**. 2007. Rhomboid protease AarA mediates quorum-sensing in *Providencia stuartii* by activating TatA of the twin-arginine translocase. Proc Natl Acad Sci U S A **104**:1003-1008.

50.   **Teixeira, J. E., and C. D. Huston**. 2008. Participation of the serine-rich *Entamoeba histolytica* protein in amebic phagocytosis of apoptotic host cells. Infect Immun **76**:959-966.

51.   **Trissl, D., A. Martinez-Palomo, M. de la Torre, R. de la Hoz, and E. Perez de Suarez**. 1978. Surface properties of *Entamoeba*: increased rates of human erythrocyte phagocytosis in pathogenic strains. J Exp Med **148**:1137-1143.

52.   **Urban, S., and M. Freeman**. 2003. Substrate specificity of rhomboid intramembrane proteases is governed by helix-breaking residues in the substrate transmembrane domain. Mol Cell **11**:1425-1434.

53.   **Urban, S., J. R. Lee, and M. Freeman**. 2001. *Drosophila* rhomboid-1 defines a family of putative intramembrane serine proteases. Cell **107**:173-182.

54.   **Urban, S., J. R. Lee, and M. Freeman**. 2002. A family of Rhomboid intramembrane proteases activates all *Drosophila* membrane-tethered EGF ligands. EMBO J **21**:4277-4286.

55.   **Urban, S., and M. S. Wolfe**. 2005. Reconstitution of intramembrane proteolysis in vitro reveals that pure rhomboid is sufficient for catalysis and specificity. Proc Natl Acad Sci U S A **102**:1883-1888.

31

56.   **Vines, R. R., G. Ramakrishnan, J. B. Rogers, L. A. Lockhart, B. J. Mann, and W. A. Petri, Jr.** 1998. Regulation of adherence and virulence by the *Entamoeba histolytica* lectin cytoplasmic domain, which contains a beta2 integrin motif. Mol Biol Cell **9**:2069-2079.

57.   **Voigt, H., and N. Guillen**. 1999. New insights into the role of the cytoskeleton in phagocytosis of *Entamoeba histolytica*. Cell Microbiol **1**:195-203.

58.   **Wang, Y., X. Guan, K. L. Fok, S. Li, X. Zhang, S. Miao, S. Zong, S. S. Koide, H. C. Chan, and L. Wang**. 2008. A novel member of the Rhomboid family, RHBDD1, regulates BIK-mediated apoptosis. Cell Mol Life Sci **65**:3822-3829.

59.   **Wasserman, J. D., S. Urban, and M. Freeman**. 2000. A family of rhomboid-like genes: *Drosophila* rhomboid-1 and roughoid/rhomboid-3 cooperate to activate EGF receptor signaling. Genes Dev **14**:1651-1663.

60.   **Yan, Z., H. Zou, F. Tian, J. R. Grandis, A. J. Mixson, P. Y. Lu, and L. Y. Li**. 2008. Human rhomboid family-1 gene silencing causes apoptosis or autophagy to epithelial cancer cells and inhibits xenograft tumor growth. Mol Cancer Ther **7**:1355-1364.

FIGURE LEGENDS

Figure 1: G3-based approach downregulates expression of EhROM1. (A)
Schematic of the G3 EhROM1 silencing construct used in our studies. 538bp of the 5'
region of EhROM1 was fused downstream of the EhAp-A cassette. **(B)** Northern blot
analysis of EhROM1 expression in G3 and ROM(KD) parasites. 20 μg of total RNA was
resolved on an formaldehyde gel and probed sequentially with probes for EhROM1 and
Lgl1, which serves as a loading control. **(C)** RT-PCR analysis of EhROM1 expression
levels in G3 and ROM(KD) parasites. 1μg cDNA from G3 and ROM(KD) cell lines were
subjected to 35 cycles of PCR for EhROM1; ssRNA is a loading control. PCR from
samples with (-)RT serve as controls to exclude genomic DNA contamination. **(D)**
Western blot analysis of EhROM1 in G3 and ROM(KD) parasites. Parasite lysates were
resolved on a 10% SDS-PAGE gel and probed with α-EhROM1 antibody (1:1000),
detected with HRP-conjugated secondary antibody (1:5000) and developed using ECL.
Blots were scanned on a Kodak Image Station 4000R.

**Figure 2: ROM(KD) parasites form caps that are morphologically
indistinguishable from G3 parasites and show no change in complement
resistance compared to G3 parasites**. Capping was induced in G3 and ROM(KD)
parasites *in vitro* by incubation of parasites with ConA on ice followed by incubation at
37−C for 15min. Parasites were then fixed and stained with anti-EhROM1 (1:20) **(A)** and
anti-Hgl (3F4, 1:30 + 7F4, 1:30) **(B)** followed by incubation with fluorescent secondary
antibodies. Parasites were stained with Texas red streptavidin (1:500) in order to image
caps (ConA contains a biotin tag). All imaging was performed on a Leica CTR6000
microscope, using a BD CARVII confocal unit. Image analysis and deconvolution was

33

performed using the LAS-AF program from Leica. De-convolution was performed in ten iterations with a single de-convolved slice shown for each sample.

Figure 3: Complement resistance and motility are not significantly altered in the ROM(KD) parasites. (A) Complement resistance was measured by incubation of trophozoites with 10% normal human serum (NHS) for 20 or 40 min at 37﹣C. Following incubation with complement, parasites were stained with 0.2% Trypan blue to assess cell viability. The average of two experiments each with a single replicate is shown with standard deviation. **(B)** Motility was measured by fluorescently labeling parasites with cell tracker dye CMFDA. Parasites were added to the upper chamber of a transwell system in serum-free medium and allowed to migrate into the lower chamber containing complete medium for 4 hr at 37﹣C. After incubation parasites in the lower chamber were quantified by reading on a fluorescence plate reader. The average of three independent experiments each with three replicates is shown with standard deviation. Data are shown as a percentage of G3 motility.

Figure 4: Rhomboid protease inhibition results in a defect in adhesion to untreated Chinese hamster ovary (CHO) cells. (A) Adhesion was measured with a CHO cell rosette assay for G3 and ROM(KD) parasites. Parasites were mixed with CHO cells at 4°C for 2 hr, after which parasites with three or more CHO cells attached were counted as positive. Data shown is an average of six experiments each with two replicates. Standard deviation is shown. *p-value <0.001. **(B)** Adhesion was measured for HM-1:IMSS parasites. The CHO cell rosette assay was modified by applying 100μM DMSO (mock control),100μM 3,4-Dichloroisocoumarin (DCI) (serine protease inhibitor with activity for rhomboid proteases) or 100μM phenylmethylsulfonyl fluoride (PMSF)

34

(serine protease inhibitor with no activity against rhomboid proteases) during the

parasite-CHO cell 2 hr incubation. Data shown is an average of two or three

independent experiments each with two replicates. Standard deviation is shown. *p-

value < 0.002.

Figure 5: No significant changes in expression levels of Gal/GalNAc lectin are

noted in the ROM(KD) parasites. (A) Microarray data from G3 and ROM(KD)

parasites was analyzed. Expression levels (average ± std deviation) for EhROM1,

EhROM2, EhROM3, EhROM4, Hgl, Igl, Lgl, and Actin are shown. The G3/ROM(KD)

fold change is shown. **(B)** Expression of Hgl and Lgl-1 transcripts were assayed by RT-

PCR and match the array data; ssRNA is a control. Microarray data has been deposited

at NCBI within the Geo Submission number GSE 21522 and NCBI tracking system

number # 15843481.

Figure 6: No significant changes in protein levels or localization of the

Gal/GalNAc lectin are noted in the ROM(KD) parasites. (A) Hgl protein expression

was measured by western blot analysis. Blots were probed with antibodies to Hgl (H85,

1:50) and Actin (1:250) as a loading control. Western blot detection was performed

using ECL. **(B)** ELISA measurement of *E. histolytica* lectin from the whole cell lysates of

G3 and ROM(KD) parasites. The parasites were lysed and the final protein

concentration adjusted to 50ng. The amount of lectin was quantified by measuring the

optical density at 450nm. **(C)** ELISA measurement of *E. histolytica* lectin from

conditioned media of G3 and ROM(KD) parasites, which was prepared by growing log-

phase trophozoites in serum-free media for 24 h. Protein concentration was adjusted to

400ng and lectin quantitated using maufacturer's instructions. Data shown as an

35

average of three independent experiments with standard deviation is shown. **(D)**
Subcellular localization of Hgl was analyzed by staining both permeabilized (P) and
nonpermeabilized (NP) parasites with anti-Hgl antibodies (3F4, 1:30 + 7F4, 1:30). All
imaging was performed on a Leica CTR6000 microscope, using a BD CARVII confocal
unit. Image analysis and deconvolution was performed using the LAS-AF program from
Leica. De-convolution was performed in ten iterations with a single de-convolved slice
shown for each sample.

**Figure 7: ROM(KD) parasites show a defect in phagocytosis of red blood cells
and rice starch. (A)** 5×10^7 hRBCs were incubated with 5×10^5 trophozoites in a ratio of
100:1 in PBS for 15 min at 37°C, followed by lysis of extracellular RBCs and
measurement of ingested erythrocytes by lysis in 90 % formic acid followed by
spectrophotometric reading at 397 nm**.** The results represent the mean and standard
deviation of four independent experiments and expressed as a percent of the parent G3
strain erythrophagocytosis. *p-value<0.001. **(B)** 1×10^5 trophozoites were incubated for
one hour with 0.004% rice starch solution following by fixation, permeabilization and
staining with 1% Lugol's solution at RT for 5 min. Parasites with one or more ingested
starch grains were considered positive for rice starch phagocytosis. Data are an
average of three independent experiments with standard deviation is shown. *p-
value<0.006.

**Figure 8: Adherence to apoptotic treated cells is not reduced in ROM(KD)
parasites but phagocytosis of these cells is decreased. (A)** Adherence to
Staurosporine treated cells is decreased in parental strain but not in ROM(KD)
parasites. CHO cells were treated either with 100μM Staurosporine aglycone or with

36

100µM DMSO for 1 h at 4°C and a CHO cell rosette assay was performed. Data are an average of three independent experiments. Standard deviation is shown. G3 (DMSO treated) versus G3 (Staurosporine treated) (*p-value<0.002); G3 (DMSO treated) versus ROM(KD) (Staurosporine treated) (*p-value<0.003). **(B)** Phagocytosis of Staurosporine treated CHO cells is decreased in ROM(KD) parasites. CHO cells were treated with 100µM Staurosporine or with 100µM DMSO for 1 h at 4°C and subsequently incubated for 15 min at 37°C with parasites (ratio 1:1). The cells were fixed, permeabilized and stained with 1% (v/v) Trichrome stain. Parasites with one or more ingested CHO cell were considered positive for phagocytosis. Data are expressed as % of G3 DMSO-treated values and are an average of three independent experiments. Standard deviation is shown. *p-value< 0.003 (DMSO treated) and *p-value< 0.007 (Staurosporine treated).

Supplementary Data

Supplementary Table 1: Microarray data for gene expression in G3 and ROM(KD) parasites. Two arrays for each strain were performed. The probe ID, fold change, gene number, annotation name, EHI number, and gene expression for G3 and ROM(KD) parasites are shown.

37

Figure 1

(A)

5' Upstream EhAp-A   5' EhROM1

473bp   538bp

(B)

G3   ROM(KD)

1.5Kb ■—   EhROM1

1.0Kb ■—   Lgl1

(C)

     G3   ROM(KD)

L +RT -RT   +RT -RT

EhROM1

ssRNA
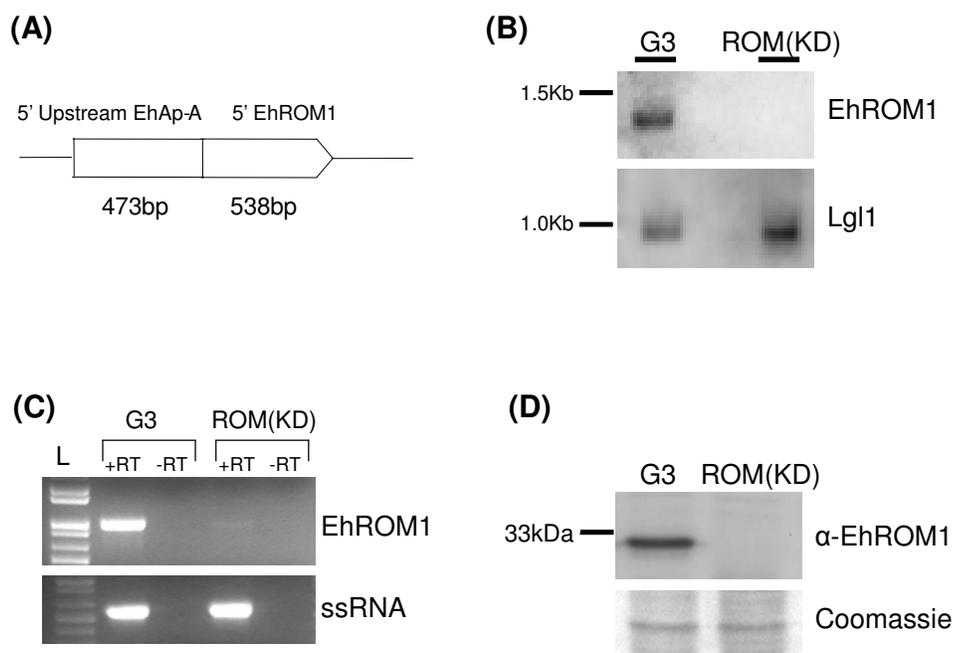
(D)

G3 ROM(KD)

33kDa ■—   α-EhROM1

Coomassie

Figure 1: G3-based approach downregulates expression of EhROM1. (A) Schematic of the G3 EhROM1 silencing construct used in our studies. 538bp of the 5' region of EhROM1 was fused downstream of the EhAp-A cassette. **(B)** Northern blot analysis of EhROM1 expression in G3 and ROM(KD) parasites. 20 μg of total RNA was resolved on an formaldehyde gel and probed sequentially with probes for EhROM1 and Lgl1, which serves as a loading control. **(C)** RT-PCR analysis of EhROM1 expression levels in G3 and ROM(KD) parasites. 1μg cDNA from G3 and ROM(KD) cell lines were subjected to 35 cycles of PCR for EhROM1; ssRNA is a loading control. PCR from samples with (-)RT serve as controls to exclude genomic DNA contamination. **(D)** Western blot analysis of EhROM1 in G3 and ROM(KD) parasites. Parasite lysates were resolved on a 10% SDS-PAGE gel and probed with α-EhROM1 antibody (1:1000), detected with HRP-conjugated secondary antibody (1:5000) and developed using ECL. Blots were scanned on a Kodak Image Station 4000R.

Figure 2 **(A)**

	ConA (cap)	α-EhROM1	Overlay
G3			
ROM(KD)			

(B)

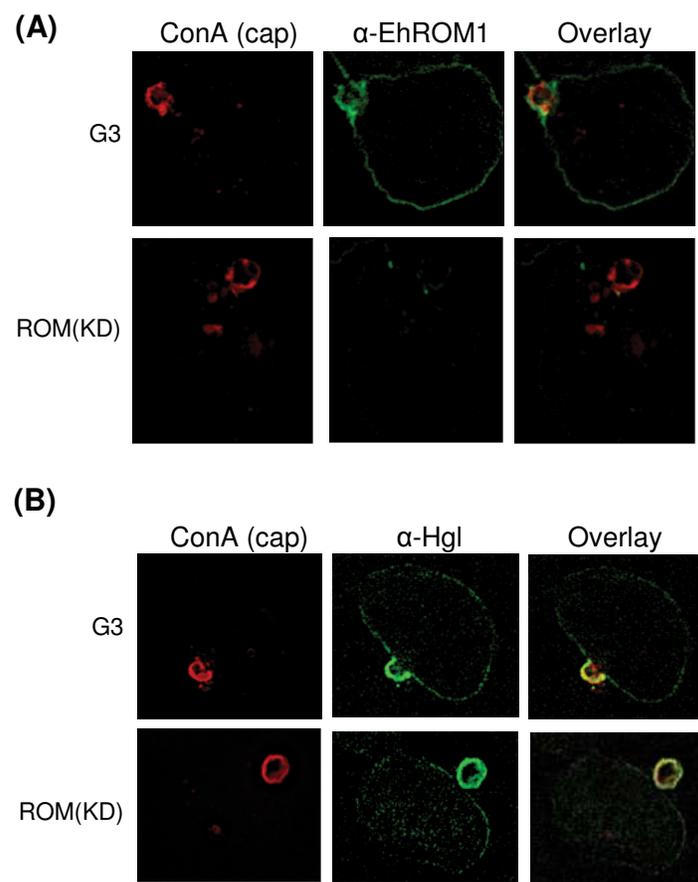|	ConA (cap)	α-Hgl	Overlay
G3			
ROM(KD)			

Figure 2: ROM(KD) parasites form caps that are morphologically indistinguishable from G3 parasites and show no change in complement resistance compared to G3 parasites. Capping was induced in G3 and ROM(KD) parasites *in vitro* by incubation of parasites with ConA on ice followed by incubation at 37−C for 15min. Parasites were then fixed and stained with anti-EhROM1 (1:20) **(A)** and anti-Hgl (3F4, 1:30 + 7F4, 1:30) **(B)** followed by incubation with fluorescent secondary antibodies. Parasites were stained with Texas red streptavidin (1:500) in order to image caps (ConA contains a biotin tag). All imaging was performed on a Leica CTR6000 microscope, using a BD CARVII confocal unit. Image analysis and deconvolution was performed using the LAS-AF program from Leica. De-convolution was performed in ten iterations with a single de-convolved slice shown for each sample.
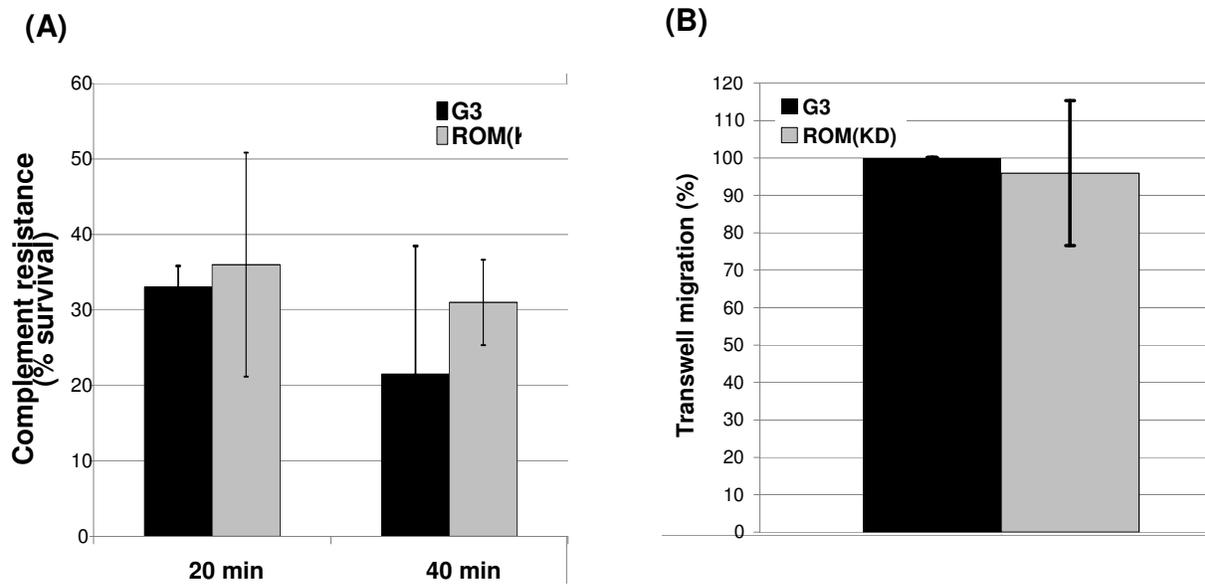
Figure 3

(A)

(B)

Figure 3: Complement resistance and motility are not significantly altered in the ROM(KD) parasites. (A) Complement resistance was measured by incubation of trophozoites with 10% normal human serum (NHS) for 20 or 40 min at 37°C. Following incubation with complement, parasites were stained with 0.2% Trypan blue to assess cell viability. The average of two experiments each with a single replicate is shown with standard deviation. **(B)** Motility was measured by fluorescently labeling parasites with cell tracker dye CMFDA. Parasites were added to the upper chamber of a transwell system in serum-free medium and allowed to migrate into the lower chamber containing complete medium for 4 hr at 37°C. After incubation parasites in the lower chamber were quantified by reading on a fluorescence plate reader. The average of three independent experiments each with three replicates is shown with standard deviation. Data are shown as a percentage of G3 motility.
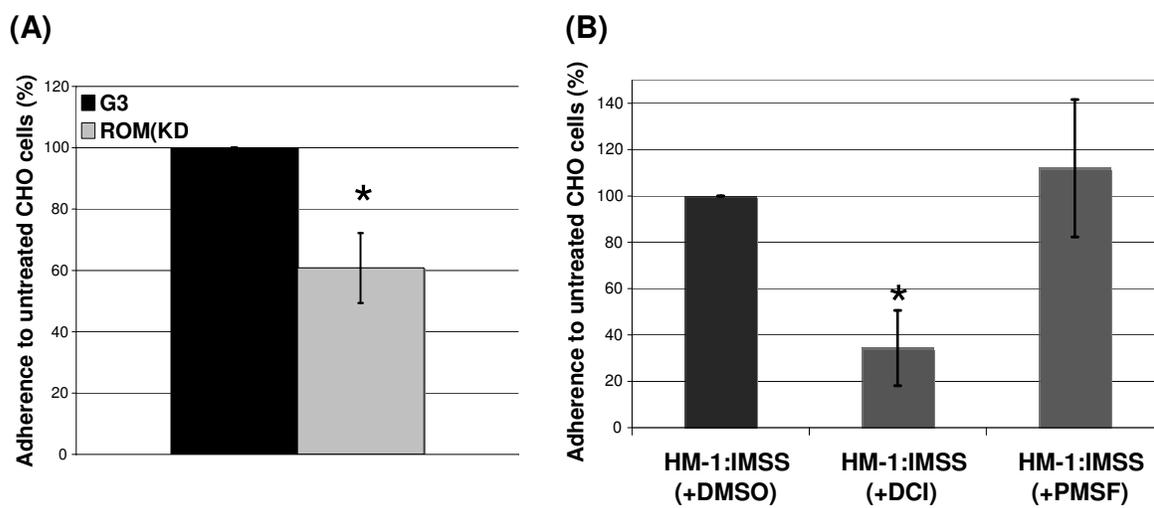
Figure 4

(A)

(B)

Figure 4: Rhomboid protease inhibition results in a defect in adhesion to untreated Chinese hamster ovary (CHO) cells. (A) Adhesion was measured with a CHO cell rosette assay for G3 and ROM(KD) parasites. Parasites were mixed with CHO cells at 4°C for 2 hr, after which parasites with three or more CHO cells attached were counted as positive. Data shown is an average of six experiments each with two replicates. Standard deviation is shown. *p-value <0.001. **(B)** Adhesion was measured for HM-1:IMSS parasites. The CHO cell rosette assay was modified by applying 100μM DMSO (mock control),100μM 3,4-Dichloroisocoumarin (DCI) (serine protease inhibitor with activity for rhomboid proteases) or 100μM phenylmethylsulfonyl fluoride (PMSF) (serine protease inhibitor with no activity against rhomboid proteases) during the parasite-CHO cell 2 hr incubation. Data shown is an average of two or three independent experiments each with two replicates. Standard deviation is shown. *p-value < 0.002.

Figure 5

(A)

	G3 (Avg ± std dev)	**ROM(KD)** (Avg ± std dev)	**Fold change**
ROM1 (EHI_197460)	33 ± 6.85	0.07 ± 0.22	**479**
ROM2 (EHI_060330)	0.33 ± 0.14	0.29 ± 0.54	1.14
ROM3 (EHI_029220)	1.65 ± 0.15	1.56 ± 0.10	1.06
ROM4 (EHI_128190)	0.93 ± 0.33	0.78 ± 0.16	1.19
Hgl (EHI_046650)	6.39 ± 3.33	7.46 ± 0.49	0.85
Hgl (no EHI number)	89.8 ± 10.97	86.08 ± 5.57	1.04
Igl (EHI_006980)	53.7 ± 39.88	40.23 ± 4.94	1.35
Igl (EHI_148790)	14.49 ± 1.03	12.28 ± 1.97	1.18
Lgl (EHI_058330)	2.86 ± 0.18	3.88 ± 0.36	0.73
Lgl (EHI_035690)	176.1 ± 2.26	177.3 ± 35.3	0.99
Actin (EHI_163580)	13.9 ± 0.34	14.6 ± 0.29	0.95

Figure 5
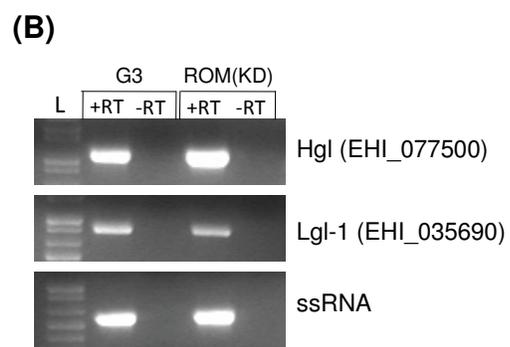
(B)

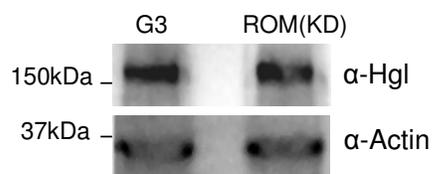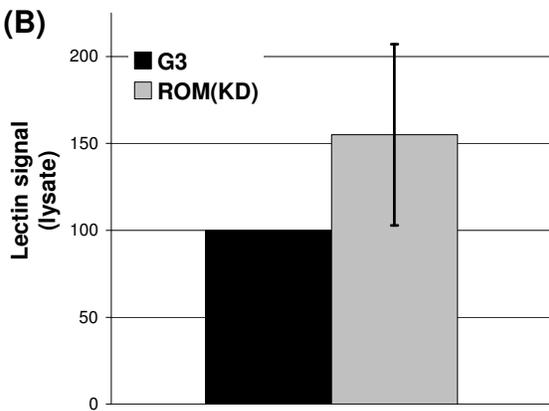|	G3	ROM(KD)	
L	+RT -RT	+RT -RT	Hgl (EHI_077500)
			Lgl-1 (EHI_035690)
			ssRNA

Figure 5: No significant changes in expression levels of Gal/GalNAc lectin are noted in the

ROM(KD) parasites. (A) Microarray data from G3 and ROM(KD) parasites was analyzed. Expression

levels (average ± std deviation) for EhROM1, EhROM2, EhROM3, EhROM4, Hgl, Igl, Lgl, and Actin

are shown. The G3/ROM(KD) fold change is shown. **(B)** Expression of Hgl and Lgl-1 transcripts were

assayed by RT-PCR and match the array data; ssRNA is a control. Microarray data has been

deposited at NCBI within the Geo Submission number GSE 21522 and NCBI tracking system number
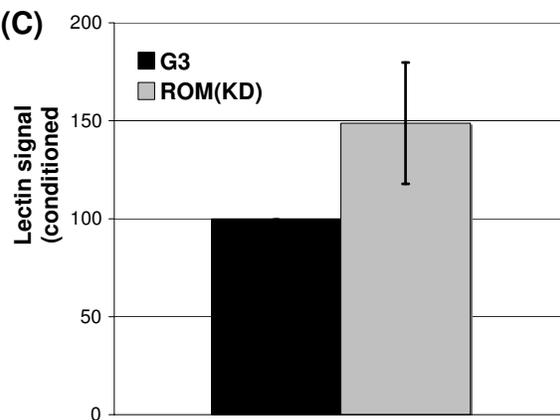
15843481.

Figure 6

(A)

(B)

(C)

Figure 6

(D)

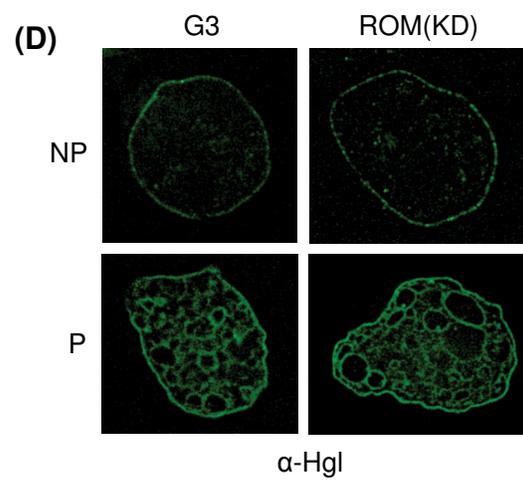G3   ROM(KD)

NP

P

α-Hgl

Figure 6: No significant changes in protein levels or localization of the Gal/GalNAc lectin are noted in the ROM(KD) parasites. (A) Hgl protein expression was measured by western blot analysis. Blots were probed with antibodies to Hgl (H85, 1:50) and Actin (1:250) as a loading control. Western blot detection was performed using ECL. **(B)** ELISA measurement of *E. histolytica* lectin from the whole cell lysates of G3 and ROM(KD) parasites. The parasites were lysed and the final protein concentration adjusted to 50ng. The amount of lectin was quantified by measuring the optical density at 450nm. **(C)** ELISA measurement of *E. histolytica* lectin from conditioned media of G3 and ROM(KD) parasites, which was prepared by growing log-phase trophozoites in serum-free media for 24 h. Protein concentration was adjusted to 400ng and lectin quantitated using maufacturer's instructions. Data shown as an average of three independent experiments with standard deviation is shown. **(D)** Subcellular localization of Hgl was analyzed by staining both permeabilized (P) and nonpermeabilized (NP) parasites with anti-Hgl antibodies (3F4, 1:30 + 7F4, 1:30). All imaging was performed on a Leica CTR6000 microscope, using a BD CARVII confocal unit. Image analysis and deconvolution was performed using the LAS-AF program from Leica. De-convolution was performed in ten iterations with a single de-convolved slice shown for each sample.
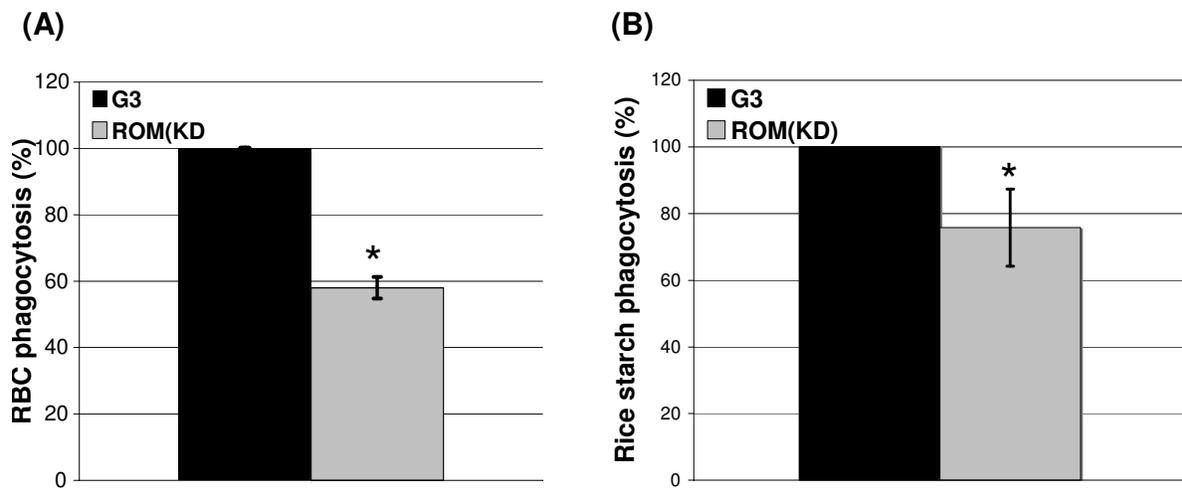
Figure 7

(A)

(B)

Figure 7: ROM(KD) parasites show a defect in phagocytosis of red blood cells and rice starch.

(A) $5X10^7$ hRBCs were incubated with $5x10^5$ trophozoites in a ratio of 100:1 in PBS for 15 min at 37℃, followed by lysis of extracellular RBCs and measurement of ingested erythrocytes by lysis in 90 % formic acid followed by spectrophotometric reading at 397 nm**.** The results represent the mean and standard deviation of four independent experiments and expressed as a percent of the parent G3 strain erythrophagocytosis. *p-value<0.001. **(B)** $1X10^5$ trophozoites were incubated for one hour with 0.004% rice starch solution following by fixation, permeabilization and staining with 1% Lugol's solution at RT for 5 min. Parasites with one or more ingested starch grains were considered positive for rice starch phagocytosis. Data are an average of three independent experiments with standard deviation is shown. *p-value<0.006.
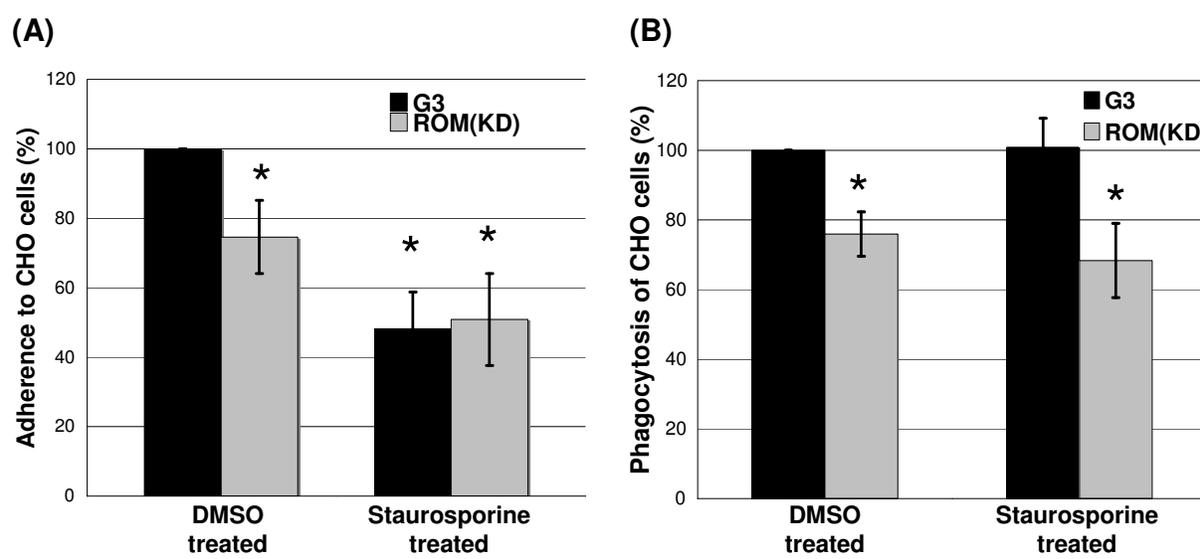
Figure 8

(A)

(B)

Figure 8: Adherence to apoptotic treated cells is not reduced in ROM(KD) parasites but phagocytosis of these cells is decreased. (A) Adherence to Staurosporine treated cells is decreased in parental strain but not in ROM(KD) parasites. CHO cells were treated either with 100µM Staurosporine aglycone or with 100µM DMSO for 1 h at 4ºC and a CHO cell rosette assay was performed. Data are an average of three independent experiments. Standard deviation is shown. G3 (DMSO treated) versus G3 (Staurosporine treated) (*p-value<0.002); G3 (DMSO treated) versus ROM(KD) (Staurosporine treated) (*p-value<0.003). **(B)** Phagocytosis of Staurosporine treated CHO cells is decreased in ROM(KD) parasites. CHO cells were treated with 100µM Staurosporine or with 100µM DMSO for 1 h at 4ºC and subsequently incubated for 15 min at 37ºC with parasites (ratio 1:1). The cells were fixed, permeabilized and stained with 1% (v/v) Trichrome stain. Parasites with one or more ingested CHO cell were considered positive for phagocytosis. Data are expressed as % of G3 DMSO-treated values and are an average of three independent experiments. Standard deviation is shown. *p-value< 0.003 (DMSO treated) and *p-value< 0.007 (Staurosporine treated).